1D image-molecular quantum states in layered media

1993 J. Phys.: Condens. Matter 5 2137

(http://iopscience.iop.org/0953-8984/5/14/011)

J. Phys.: Condens. Matter 5 (1993) 2137–2142. Printed in the UK

1D image-molecular quantum states in layered media

M Babiker
Department of Physics, University of Essex, Colchester CO4 3SQ, UK

Received 4 November 1992

Abstract. A charge carrier in a layered system experiences an additional Coulomb potential due to its interaction with its own set of images. The latter arise due to the differences between the dielectric properties of the layer materials. The charge can, further, form bound quantum states in its own image potential. The physical situation is examined here for a double heterostructure. It is first shown that for sufficiently large layer thicknesses, depending on the layer materials, the ground state exhibits image-molecular features. Qualitatively, such features are explainable largely in terms of the overlap between the first-order image-induced states due to two separate interfaces. This is further substantiated by the numerical solution of the Schrödinger equation which provides predictions for a wide range of layer thicknesses by taking account of the multiple images.

It is well known that dynamical image charges are induced whenever real charges move near the interface between two dissimilar media. The interaction between the charge and its own image system can, in principle, trap the particle in one of a series of quantum energy levels. The prototype of such quantum states are those observed at the liquid helium/vacuum interface as reported long ago by Grimes *et al* [1].

The scope of the physics of such a situation is considerably widened by the advent of layered microstructures involving insulators, semiconductors, metals and semimetals [2]. A typical requirement of a layered microstructure system is the formation of quantum wells due to abrupt changes in conduction or valence band edges at the abrupt material interfaces. The characterization of quantum well states, especially the ground state, thus formed, due to band edge discontinuities, is now considerably advanced, so much so that quantum well lasers are engineered with specific requirements based on supposedly well defined quantum well attributes.

It is precisely because microstructures offer a wide range of possibilities, in terms of material combinations and parameters, that we examine here the significance of image-type effects in that context and the possibility of their modifying the optical and electronic characteristics of such systems. It turns out that, besides expected modifications to characteristic energies, the problem exhibits some new features which are worthy of special emphasis.

Consider therefore a double heterostructure composed of a layer of material 1 sandwiched between two much thicker layers of material 2. The complete image potential for an electron inside layer 1 is obtained simply by summing up contributions from multiple images to all orders. We have

$$V_i(z) = -\frac{e_0^2}{4}\sum_{k=0}^{\infty}\left\{\frac{\gamma^{2k+1}}{z+kL} - \frac{2\gamma^{2(k+1)}}{L(k+1)} + \frac{\gamma^{2k+1}}{(k+1)L-z}\right\} \qquad (1)$$

0953-8984/93/142137+06$07.50

where $z(0 < z < L)$ is the position of the particle relative to one of the interfaces γ is given by

$$\gamma = (\epsilon_1 - \epsilon_2)/(\epsilon_2 + \epsilon_1) \tag{2}$$

with ϵ_1 and ϵ_2 the electric permittivities of materials 1 and 2, respectively, where we assume that $\epsilon_2 > \epsilon_1$. The quantity e_0 is defined by

$$e_0^2 = e^2/4\pi\epsilon_1 \tag{3}$$

and L is the layer width of material 1.

In a typical double heterostructure, material 1 would be a semiconductor with a lower band gap than material 2. Then in the absence of any image effects the potential in material 1 is taken as V_c corresponding to the bottom of the conduction band for electrons. The complete potential including quantum well image effects is therefore given by

$$V_L = V_i + V_c \tag{4}$$

and the required states are obtainable by the solution of the one-dimensional Schrödinger equation

$$-(\hbar^2/2m^*)\partial^2\psi_n(z)/\partial z^2 + V_L(z)\psi_n(z) = W_n\psi_n(z) \tag{5}$$

where m^* is the effective mass in material 1, where the particle is confined. Since exact analytical solutions of equation (5) do not exist, we are forced to resort either to approximation methods or make use of numerical techniques. In what follows we first seek an approximate analytical solution and then we describe the results of the numerical method.

Consider first a physically transparent initial approximation in which the width L is assumed to be sufficiently large that the physics of the situation can be viewed as predominantly due to the two separate interfaces. The motion of the charged particle is then determined primarily by the first-order image approximation which corresponds to the potential in equation (1) having only the three leading terms, two (first order in γ) arising from the interaction of the particle charge with its two first images and a third term (second order in γ) is the interaction between the first-order images. Note that the first-order images are always separated by a distance 2L irrespective of the position z of the real charge. We write

$$V_L(z) = V_c - \left(e_0^2\gamma/4\right)[1/z + 1/(L - z)] + e_0^2\gamma^2/2L. \tag{6}$$

The situation is reminiscent of the well known two-centre problem of the hydrogen molecule ion. In the present case one-dimensional case each centre corresponds to an interface and we need therefore to outline the formalism and results for the single-interface eigenproblem. For motion near the interface at $z = 0$ we have

$$-(\hbar^2/2m^*)\partial^2\phi_n/\partial z^2 + \left(V_c - e_0^2\gamma/4z\right)\phi_n = E_n\phi_n \tag{7}$$

and for that near the interface $z = L$ we have an identical equation by writing $L - z = \xi$ instead of z. The exact solutions of equation (7) are well known [3]. We have the eigenenergies

$$E_n = V_c - e_0^2\gamma^2/32a^*n^2 \tag{8}$$

where a^*, defined by

$$a^* = \hbar^2/m^*e_0^2 \tag{9}$$

is an effective Bohr radius, which we shall adopt as a convenient length scale of the problem. The ground-state eigenfunction corresponding to E_1 is given explicitly by

$$\phi_1(z) = 2(\gamma/4a^*)^{3/2} z \exp(-z\gamma/4a^*). \tag{10}$$

For orientation as to the order of magnitude for the ground state E_1 and the effective Bohr radius a^* we consider two different cases of the single heterostructure.

(A) The vacuum/perfect conductor case corresponds to $\gamma = 1$; $\epsilon_1 = \epsilon_0$ and $m^* = m_e$. We have

$$E_1 = V_c - 850 \text{ meV} \qquad a^* = a_B \tag{11}$$

where a_B is the conventional Bohr radius. The electron moving in vacuum near the perfect conductor surface is thus tightly bound to the surface. We can also check that the expectation value of z in the ground state is $\langle z \rangle_{\phi_1} = 4a_B$. In practice the average surface roughness introduces a length scale which is larger than a_B.

(B) The semiconductor/metal interface corresponds to the choice

$$\gamma \simeq 1.0 \qquad m^* \simeq 0.5 m_e \qquad \epsilon_1 = 10\epsilon_0. \tag{12}$$

We have in this case

$$E_1 = V_c - 4.1 \text{ meV} \tag{13}$$

$$a^* = a_B\left(\epsilon_1 m_e/\epsilon_0 m^*\right) \simeq 20 a_B \tag{14}$$

$$\langle z \rangle_{\phi_1} = 4a^*/\gamma \simeq 40 \text{ Å}. \tag{15}$$

Clearly the electron in this latter case is weakly bound to the surface with a ground-state energy about 4 meV below the conduction band edge, and the average distance can be safely assumed to be much larger than a typical surface roughness length.

An approximate solution of equation (5), appropriate for the ground state of the double heterostructure, is obtained by writing $\psi_1(z)$ as a linear combination of single interface functions $\phi_1(z)$ and $\phi_1(L - z)$:

$$\psi_1(z) = c_0\phi_0(z) + c_L\phi_L(z) \tag{16}$$

where

$$\phi_0 = \phi_1(z) \qquad \phi_L = \phi_L(L - z). \tag{17}$$

We seek the symmetric solution (corresponding to $c_0 = c_L$) by analogy with the hydrogen molecule ion case [4]. We find

$$W_1^a = (H_{00} + H_{0L})/(1 + S) + V_c + e_0^2\gamma^2/2L \tag{18}$$

where

$$H_{00} = \langle \phi_0 | H | \phi_0 \rangle \qquad H_{0L} = \langle \phi_0 | H | \phi_L \rangle \tag{19}$$

with

$$H = p_z^2/2m^* - \left(e_0^2\gamma/4\right)\left[1/z + 1/(L - z)\right]. \tag{20}$$

S is the overlap integral in the region $0 \leqslant z \leqslant L$:

$$S = \langle \phi_0 | \phi_K \rangle. \tag{21}$$

Straightforward evaluations of the integrals yield for W_1^a

$$W_1^a(L) = V_c + \frac{e_0^2\gamma^2}{2L} - \left(\frac{e_0^2\gamma^2}{32a^*}\right)\left[1 + \frac{8a^*G}{\gamma L} + S + \frac{L^2\gamma^2}{4a^{*2}}\exp\left(\frac{-\gamma L}{4a^*}\right)\right]\Big/(1+S) \tag{22}$$

where

$$G = 1 - \exp(-L\gamma/2a^*)(1 + L\gamma/2a^* + \gamma^2L^2/8a^{*2}) \tag{23}$$

$$S = (\gamma^3L^3/96a^{*3})\exp(-L\gamma/4a^*). \tag{24}$$

Clearly as $L \to \infty$, we have $W_1^a \to E_1$, where E_1 is given by equation (8).

It therefore seems appropriate to argue along the hydrogen molecule ion lines and speak of an image molecule composed of the electron in the fields of its two first-order images. The above result, equation (22), gives W_1^a as the first approximation of the ground-state energy of such an image molecule as a function of the layer width L. Like the hydrogen molecule ion case one expects a minimum to occur at some value of L, $L(\min)$, corresponding to stable equilibrium. The minimum value of the ground-state energy predicted by the current approximation, as shown in figure 1, suggests that a stronger binding of the electron results from the process of overlapping of the first-order image effects at finite layer thickness. Although the analytical approximation method used above is physically transparent and has led to the prediction of the image-molecule-type features shown in figure 1, any quantitatively useful predictions would need more accurate solutions of the problem.

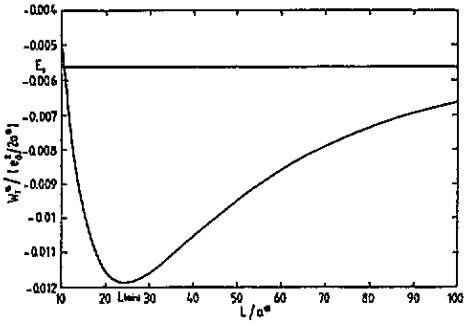

Figure 1. Variation of the (γ = 0.3) approximate ground-state energy W_1^a with layer width L. Energy is measured in units of half and affective Rydberg ($e_0^2/2a^*$) and lengths in units of a^*. The dashed horizontal line is the asymptote $L \to \infty$ where $W_1^a \to E_1 = \gamma^2/16$. The bottom of the conduction band V_c corresponds to zero energy.

We have, therefore, adopted numerical methods to solve equation (5) including higher-order image contributions, as given in equation (1). The results displayed in figure 2(*a*) and 2(*b*) are those for particular values of γ: figure 2(*a*) has γ = 1.0 and figure 2(*b*) has γ = 0.3. It is seen that for both values of γ the ground-state energy for this more accurate evaluation does indeed exhibit the important qualitative feature emerging from the previous method, namely the image-molecule-type effects indicated by the appearance of an energy minimum. The results suggest that higher-order image effects can contribute significantly to the binding energy and determine more accurately the value of $L(\min)$. The manner in which the overlap manifests itself as L is decreased is shown in figure 3, which traces the ground-state probability distributions for the case γ = 0.3 (corresponding for figure 2(*b*)) from a large value of L, exhibiting quasi-independent interface effects to the region near the minimum, where overlap effects are significant. Figures 2(*a*) and 2(*b*) also exhibit the variations

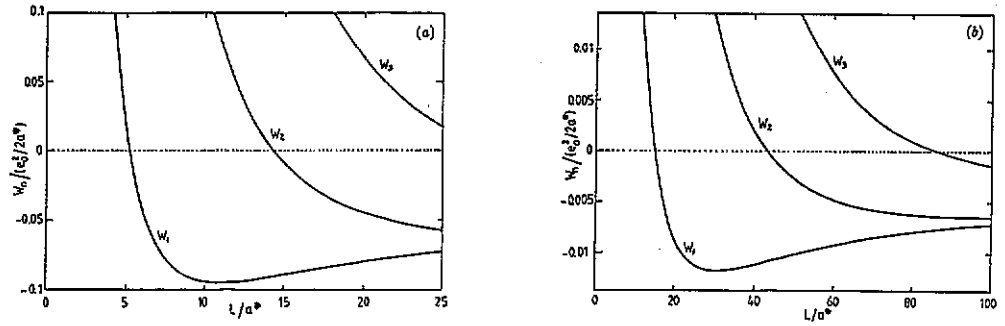

Figure 2. Variation with L of the lowest three eigenvalues of the Schrödinger equation (5) evaluated numerically for the cases (*a*) $\gamma = 1.0$ and (*b*) $\gamma = 0.3$. The energy and length scales are as defined in the caption to figure 1.

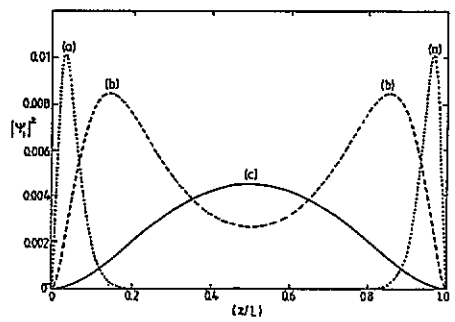

Figure 3. Unnormalized ground-state probability distributions for the case $\gamma = 0.3$ and for ($L = 400a^*$ curve a), ($L = 100a^*$ curve b), ($L = 20a^*$ curve c).

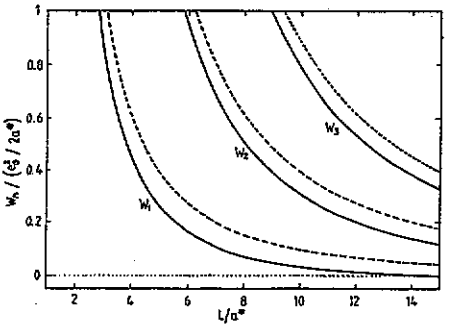

Figure 4. Variations in the region of small L of the three lowest eigenvalues of equation (5) evaluated numerically for the case $\gamma = 0.3$ as shown by the full curves. These curves are, therefore, small-L extensions of those in figure 2(*b*). The dotted curves are the corresponding energy eigenvalues in the absence of image effects.

of W_2 and W_3 with L. Clearly in the regions of variation shown all three lowest-energy states have values below the conduction band minimum. This is a marked departure from the usual quantum well states in the absence of image effects.

Figure 4 displays for the case $\gamma = 0.3$ the variation of W_1, W_2 and W_3 in a region of smaller L (where all energies are above the conduction band minimum) and compares these with the corresponding variation of the conventional quantum well energies obtainable analytically in the absence of image effects (equivalent to setting $\gamma = 0$ throughout). We have

$$W_n(\gamma = 0) = (a^{*2}n^2\pi^2/L^2)(e_0^2/2a^*) + V_c. \tag{25}$$

It is seen from figure 4 that the image effects can produce important modifications of the lowest eigenenergies in this region of small L, depending on the type of heterostructure. For example, for $L = 4.0a^*$ changes of the order of 30% in the ground-state energy can arise due to such image effects. In the example represented by the parameters given in equation (12) $L \simeq 4a^*$ corresponds to $L \simeq 40$ Å which is a

typical quantum well width. It must therefore be emphasized that the small L region refers to small values of the ratio L/a^*, which could be small or large depending on the value of a^*. The present treatment should be appropriate for small values of L/a^* provided that a^* is sufficiently large.

In conclusion we have investigated the effects of the self-image contribution on the confinement of charged carriers in double heterostructures. The results show that, in general, image effects can contribute significantly to the properties of charged carriers in such structures. An interesting feature of the results is the prediction of $L(\min)$ for a given pair of materials and the way in which the ground state exhibits the image-molecular characteristics discussed above. The effects are clearly enhanced in absolute terms for pairs of materials resulting in (i) a relatively large value of γ, (ii) a moderately large value of the carrier effective mass m^*, and (iii) a relatively small dielectric permittivity of the layer. These criteria imply that image effects are likely to be small in alloy III–V semiconductor structures (for example GaAs/GaAlAs) which exhibit small γ and m^* and a relatively large permittivity for GaAs. By contrast the effects appear to be important for cases of free-standing structures such as Si/vacuum and also for semiconductor/metal and semiconductor/insulator pairs for which some (if not all) of the above three criteria are satisfied.

In the recent literature interest in image charges in heterostructures has concentrated primarily on the modifications they cause to exciton binding energies [5,6] and to impurity levels [7–9] as the layer width L varies. Such changes are brought about by a combination of self-image interactions and image-modified inter-particle interactions. The existence of characteristic layer widths $L(\min)$ of the type discussed in this paper for single charges suggests that analogous effects should be exhibited in the cases of excitons and hydrogenic impurity levels in heterostructures. Investigations along these lines are now in progress.

Acknowledgment

The author is grateful to Sue Babiker for her expert help with the computational aspects of this work.

References

[1] Grimes C C, Brown T R, Burns M L and Zipfel C L 1976 *Phys. Rev.* B **13** 140
[2] Weisbuch C and Vinter B 1991 *Quantum Semiconductor Structures* (New York: Academic)
[3] Babiker M and Tilley D R 1981 *Proc. R. Soc.* A **378** 369
[4] Atkins P W 1992 *Molecular Quantum Mechanics* 2nd edn (Oxford: Clarendon)
[5] Tran Thoai D B, Zimmermann R, Grundman M and Bimberg D 1990 *Phys. Rev.* B **42** 5906
[6] Wendler L and Hartwig B 1991 *J. Phys.: Condens. Matter* **3** 9907
[7] Green R L and Bajaj K K 1983 *Solid State Commun.* **45** 825
[8] Shanabrook B V 1987 *Physica* B **146** 121
[9] Wendler L and Hartwig B 1990 *J. Phys.: Condens. Matter* **2** 8847